# Unraveling Excited States of Doped Helium Clusters[†]

## Tatjana Škrbić,[£] Saverio Moroni,* and Stefano Baroni[‡]

*SISSA—Scuola Internazionale Superiore di Studi Avanzati, and CNR-INFM DEMOCRITOS National Simulation Center, via Beirut 2-4, 34014 Trieste, Italy*

We discuss the use of generalized, symmetry-adapted, imaginary-time correlation functions to study the rotational spectrum of doped helium clusters within the frame of the reptation quantum Monte Carlo method. Analysis of these correlation functions allows one to enhance the computational efficiency in the calculation of weak spectral features, as well as to get a qualitative insight into the nature of the different lines. The usefulness of this approach is demonstrated by a study of the He−CO binary complex, used as a benchmark case, as well as by preliminary results for the satellite band recently observed in the IR spectrum of the $CO_2$ molecule solvated in He nanodroplets.

The spectroscopic interrogation of molecules individually embedded in superfluid He nanodroplets, pioneered by Scoles in the early 90s,[1] has spawned an ever increasing number of experimental and theoretical works aimed at elucidating the interplay between the molecular rotational and vibrational features of the spectrum and the structure of the He matrix.[2−5] One of the most spectacular features that emerges from the resulting rich phenomenology is the free-rotor character of the rotational spectrum, with a molecular inertia that is increased with respect to its gas-phase value. This behavior is intimately related to the most fundamental physical property of the quantum solvent, namely, its superfluid character, which persists down to extremely small system sizes.[6,7] Superfluidity (which can be traced back to the scarcity of low-energy excitations in this confined interacting boson system), together with the mildness of the He−molecule interaction, makes He droplets, in a sense, the ultimate spectroscopic matrix.[8]

While considerable progress has been made in the understanding of the fundamental properties of these systems (such as, e.g., their structure and its relation to superfluidity, the turnaround between a classical to a superfluid behavior of the host, as a function of the system size, etc.), many subtle features of the observed spectra still remain to be understood. For instance, the residual interaction between the effective rotor (constituted by the molecule together with part of the He density dragged around by it) and the rest of the host gives rise to such phenomena as line broadening and splitting and satellite bands (faint spectral features that would be absent in the spectrum of a rigid rotor), which still escape a proper theoretical understanding. Examples of these effects include the splitting of the R(0) lines in the spectra of small CO@He$_N$ clusters,[11] as well as the satellite band that is observed to accompany the strong and sharp R(0) rovibrational line in the infrared spectra of He-solvated $CO_2$.[12]

Much of this progress is due to recent advances in the quantum simulation technology that is currently capable of providing microscopic information not easily accessible (or not

accessible at all) to experiment. Thanks to these advances, the scope of quantum Monte Carlo simulations of interacting bosons is being extended from the structure of the ground state to the dynamical regime, at least in the low-frequency portion of the spectrum.[10] As a result, a deep insight is being gained into the physical mechanisms responsible for superfluidity in doped He clusters and nanodroplets and its manifestation in their rotational spectrum, in terms of the interplay between structure and dynamics, localization, and tunneling.[9] The main theoretical tool employed in these investigations is the dipole−dipole imaginary-time correlation function (CF), whose inverse Laplace transform (ILT) displays peaks in correspondence to dipole-allowed electromagnetic transitions, with strengths proportional to the transition matrix elements between the ground and the excited states. Imaginary-time CFs are easily accessible to reptation quantum Monte Carlo (RQMC) simulations without any other systematic biases than those due to the use of a finite time step and propagation time.[10] The main effect of the residual interactions between the effective rotor and the rest of the host is that the spectrum is not entirely exhausted by the renormalized $J = 1$ molecular rotation, thus indicating the presence of additional, weaker spectral features higher in energy. The strength of these additional features, however, may be so weak as to make them hardly detectable through the numerically instable and ill-conditioned ILT operation. The main purpose of this work is to show how the use of generalized, symmetry-adapted, imaginary-time correlation functions allows one to selectively enhance the weight of faint spectral features, thus making them accessible to the analysis of the ILT. As a demonstration of our methodology, we apply it to the He−CO dimer, for which exact diagonalization results are available, and we present preliminary results for the simulation of the satellite band recently observed in the IR spectrum of the $CO_2$ molecule solvated in He nanodroplets.[12]

The absorption spectrum of a molecule embedded in a matrix of helium atoms is given by the Fourier transform of the time autocorrelation of its dipole **d**. At zero temperature, one has

$$I(\omega) \sim \sum_i |\langle \Psi_i | \hat{\mathbf{d}} | \Psi_0 \rangle|^2 \delta(E_i - E_0 - \omega) = \int \langle \hat{\mathbf{d}}(t) \cdot \hat{\mathbf{d}}(0) \rangle_0 e^{i\omega t} dt \quad (1)$$

* To whom correspondence should be addressed. E-mail: moroni@democritos.it.
£ E-mail: skrbic@sissa.it.
‡ E-mail: baroni@sissa.it.

where $\Psi_i$ and $E_i$ are the eigenfunctions and eigenvalues of the Hamiltonian, $|\langle\Psi_i|\hat{\mathbf{d}}|\Psi_0\rangle|^2$ is the oscillator strength of the $0 \rightarrow i$ transition, and $\langle\cdot\rangle_0$ denotes a ground-state expectation value. The spectrum can be also obtained from the ILT of the imaginary-time autocorrelation of $\hat{\mathbf{d}}$

$$\mathcal{C}(\tau) = \langle\hat{\mathbf{d}}(\tau)\cdot\hat{\mathbf{d}}(0)\rangle_0 = \sum_i |\langle\Psi_i|\hat{\mathbf{d}}|\Psi_0\rangle|^2 e^{-(E_i-E_0)\tau} \quad (2)$$

This is computationally convenient because $\mathcal{C}(\tau)$ can be readily calculated with quantum Monte Carlo (QMC).[9,10,14] Although, in general, the inversion of a Laplace transform is a numerically instable and ill-conditioned procedure,[14] it does yield reliable results when the spectrum is exhausted by a few, well-separated lines, which is often the case for the rotational energies of molecules solvated with He atoms. When these favorable conditions are met, the results are largely independent of whether the ILT is accomplished, for instance, by a multiexponential fit[15]—the procedure adopted in this work—or by a maximum entropy analysis.[18] On the other hand, upon proliferation of excited states and/or a decrease of their spectral weights, the ILT results tend to become ambiguous: the statistical noise grows, and it becomes increasingly difficult to avoid systematic bias.

Using realistic Hamiltonians, accurate QMC simulations of doped clusters containing up to a few tens of He atoms have indeed given significant insight into the interplay among structure and superfluidity of the solvent and the rotational dynamics of molecules soluted in He clusters and nanodroplets.[9,15] For example, a recent infrared study[11] has shown that the a-type and the b-type rotational modes of the binary CO–He complex evolve into two series of R(0) transitions as the number $N$ of He atoms increases. The former starts with low intensity, then gradually gains spectral weight, and eventually outlasts the latter for $N$ larger than about 10. RQMC simulations[15] explain the presence of two series and the disappearance of one of them before completion of the first solvation shell, in terms of structural properties of the He solvent surrounding the molecule. Furthermore, analysis of the quantum simulation data indicates that the a-type mode starts with a strong end-over-end character—a result that is well-known in the case of the binary complex[16,17]—and then gradually acquires both relative intensity and free-rotor character, heading toward the nanodroplet limit. This result was achieved from the analysis of the imaginary-time CF of the unit vector $\hat{\mathbf{u}}$ in the direction of the He center of mass, $\mathcal{C}_u(\tau) = \langle\hat{\mathbf{u}}(\tau)\cdot\hat{\mathbf{u}}(0)\rangle_0$. The oscillator strengths extracted from the spectral decomposition of $\mathcal{C}_u$ can be taken as a measure of the end-over-end character of the excited states with total angular momentum $J = 1$, whereas a similar analysis of $\mathcal{C}$ gives information about the free-rotor character of the $J = 1$ states. For instance, the a-type mode of the binary complex is a mixed end-over-end and free-rotor state because its oscillator strength is sizable in both $\mathcal{C}(\tau)$ and $\mathcal{C}_u(\tau)$.[15] Furthermore, we can deduce that the character of this excitation is mainly end-over-end because this state carries nearly all of the spectral weight in $\mathcal{C}_u(\tau)$ but only $\approx$10% in $\mathcal{C}(\tau)$. The energy of this state can be located from the analysis of either CF. However, because of the larger spectral weight and the ill-conditioned property of the ILT, it is easier and more accurate to extract this energy from the spectral decomposition of $\mathcal{C}_u$ rather than from $\mathcal{C}$. We thus see that the choice of a suitable CF not only gives physical information on the character of a given excited state but can also lead to improved computational efficiency.

The above example shows the potential reach of suitably defined CFs for a deeper understanding and/or a faster calcula-

tion of specific spectral properties. In this paper, we define a larger set of CFs and explore their usefulness by giving preliminary results for a couple of test cases.

We consider a rigid linear rotor X, with the molecular axis along the $\hat{\mathbf{n}}$ direction. The $i$th He atom has coordinates $\mathbf{r}_i$ with respect to the center of mass of the molecule. Furthermore, we restrict ourselves to the $J = 1$ sector of the spectrum and will drop the $J$ index unless really needed. Since we are interested in the rotational spectrum of the doped cluster, we build our CFs using angular variables only. The total angular momentum of the system is conserved, whereas the angular momentum of the molecule and the sum of the atomic angular momenta are not. The eigenstates of the Hamiltonian, which can be chosen as eigenstates of the total angular momentum, can therefore be formally expanded into sums of products of eigenstates of the molecular angular momentum, $\phi_{jm_j}^X$, and of the total atomic angular momentum, $\phi_{lm_l}^{He}$

$$\Psi_{JM} = \sum_{j,m_j,l,m_l} \phi_{jm_j}^X \otimes \phi_{lm_l}^{He} \langle jm_j, lm_l|JM\rangle \quad (3)$$

where $\langle lm_l, jm_j|JM\rangle$ are Clebsch–Gordan coefficients (CGCs). Since the total angular momentum of the cluster in the ground state is zero, the only CGCs giving a nonvanishing contribution to the sum have $j = l$ and $m_j = -m_l$: $\langle lm_l, l - m_l|00\rangle$. Likewise, an excited state with $J = 1$ will have factors with $|l - 1| \leq j \leq l + 1$ and the corresponding CGCs. Optically allowed excited states will have $J = 1$. These states can be coupled to the ground state through an irreducible tensor operator of rank $J = 1$. Irreducible tensor operators can be decomposed into sums of tensor products of operators acting on the molecular and atomic components of the Hilbert space of cluster states, analogous to the decomposition of states themselves, eq 3

$$\mathcal{T}_{JM} = \sum_{j,m_j,l,m_l} t_{jm_j}^X \otimes t_{lm_l}^{He} \langle jm_j, lm_l|JM\rangle \quad (4)$$

where $t^{He(X)}$ are irreducible tensor operators acting on the atomic (molecular) components of the cluster Hilbert space. Among the many different possibilities for the $t^{X,He}$ operators, we can choose diagonal operators in the coordinate representations, such as $t_{jm_j}^X(\hat{\mathbf{n}}) = Y_{jm_j}(\hat{\mathbf{n}})$ and

$$t_{lm_l}^{He}(\{\mathbf{r}_i\}) = \frac{1}{N}\sum_i Y_{lm_l}(\hat{\mathbf{r}}_i)$$

where the $Y$'s are spherical harmonics. Note that the $\phi_{00}^{He} \otimes \phi_{00}^X$ component of the ground state is coupled to the $\phi_{lm_l}^{He} \otimes \phi_{jm_j}^X$ component of an optically allowed excited-state by the $\mathcal{T}_{1M}^{jl}$ component of the expansion of eq 4, defined as

$$\mathcal{T}_{1M}^{jl} = \sum_{m_j,m_l} Y_{jm_j}^X(\hat{\mathbf{n}}) t_{lm_l}^{He}(\{\mathbf{r}_i\}) \langle jm_j, lm_l|1M\rangle \quad (5)$$

Finally, we define symmetry-adapted, imaginary-time correlation functions (SAITCFs) as

$$\mathcal{C}_{jl}(\tau) = \left\langle \sum_{M=-1}^{1} \mathcal{T}_{1M}^{jl*}(\tau) \mathcal{T}_{1M}^{jl}(0) \right\rangle_0 \quad (6)$$

The idea of using different coupling operators to probe different excited states is not new. In the projection operator imaginary time spectral evolution (POITSE) approach,[13] for instance, it has been used to separate rotations and vibrations

**TABLE 1**[a]

|  | (0,1) | | (1,0) | | (1,1) | | (1,2) | |
|---|---|---|---|---|---|---|---|---|
|  | *E* | *A* | *E* | *A* | *E* | *A* | *E* | *A* |
| $\mathscr{C}_{01}$ | 0.5810(8) | 0.969(2) |  |  |  |  | 8.0(6) | 0.0171(7) |
| $\mathscr{C}_{10}$ | 0.58(2) | 0.119(4) | 4.09(3) | 0.861(4) |  |  |  |  |
| $\mathscr{C}_{11}$ |  |  |  |  | 4.322(13) | 0.974(3) |  |  |
| $\mathscr{C}_{12}$ | 0.612(14) | 0.113(2) |  |  |  |  | 6.07(6) | 0.810(8) |
| exact | 0.5817 | 0.9126 | 4.0175 | 0.9002 | 4.3079 | 0.9807 | 6.1049 | 0.8308 |

[a] The RQMC energies, $E$ (in $cm^{-1}$) and spectral weights, $A$, of each of the four bound states of the He−CO dimer, labeled $(j,l)$ as obtained from the $\mathscr{C}_{ik}$ correlation function. For the empty entries, the spectral weight is either zero or too small to be detected. The last row lists the exact results of refs 20 and 21. Note that $A$ has a different meaning for the exact calculation and for RQMC; in the former case, it is the contribution of the dominant $(j,l)$ component in the exact eigenstate; in the latter, it is the weight of that particular eigenstate in the spectral decomposition of $\mathscr{C}_{ik}$.

of a model He−X binary complex. We believe that application of these ideas to the much more powerful and numerically stable RQMC framework will open the way to a much better understanding of weak spectral features in doped He clusters and nanodroplets.

An alternative strategy is the explicit construction of accurate wave functions for excited states. This exceedingly difficult task can yield good results in particular cases, but it is unlikely to be a viable approach in general. For example, remarkable results have been recently obtained[19] for the nodal structure of rotational states in very small clusters, but the extension to large systems is not straightforward and seemingly requires some ad hoc processing.

Our first application is a test against known results, namely, the rotational spectrum of the binary complex He−CO, as described by a potential energy surface calculated with symmetry adapted perturbation theory (SAPT).[20,21] For the technical aspects of the simulation, we refer to previous work.[9,15,22] For the binary complex, the full spectrum can be obtained exactly by a converged variational calculation.[20,21] The He−CO potential energy surface supports four bound states with $J = 1$, which can be classified with the molecule and He angular momenta, $j$ and $l$, respectively. Although they are not good quantum numbers, the dominant $(j,l)$ contribution in each of these bound states is about 90%. The exact calculation and the RQMC results are listed in Table 1. The simulation should also give unbiased results, and indeed, we observe a good agreement between the exact results and the RQMC excitation energies, with only a few small discrepancies due to the mentioned weaknesses of the ILT. For instance, the (1,0) state is the second lowest in the $\mathscr{C}_{10}(\tau)$ CF, which further contains higher excitations; this is a rather complex situation, and we consider the agreement quite gratifying.

We stress that when using the "standard" dipole−dipole correlation function, $\mathscr{C}_{10}(\tau)$, only the (1,0) and (0,1) excitations—among the bound states—have a sufficient spectral weight to be detected in the calculation (see ref 15 and Table 1). Using more CFs, instead, we can resolve all four bound states. Of course, spectral features that are weak or even missing in a particular correlation function are not necessarily so in a different one. As we already know from ref 15, the energy of the a-type (0,1) state can be extracted not only from $\mathscr{C}_{10}$ (which gives, in the present simulation, $0.58 \pm 0.02$ $cm^{-1}$) but also—with much higher precision—from $\mathscr{C}_{01}$ (see Table 1). Using the new SAITCFs, we further see that the end-over-end mode (0,1) is present also in $\mathscr{C}_{12}$, with an estimated energy of $0.612 \pm 0.014$ $cm^{-1}$. The $\mathscr{C}_{11}$ CF, instead, remains on its own, despite the closeness of the energy of its dominant contribution, (1,1), with the free-rotor mode. This is due to the even parity of the (1,1) state, different from all of the other three bound states.

We conclude this discussion of the He−CO rotational excitations by briefly mentioning preliminary calculations of

the evolution of all four bound states with the number of He atoms. They indicate that the difference in energy between the (1,0) and the (1,2) states is smallest at $N \approx 6$. There is an intriguing possibility that the CFs discussed in this work can explain the line splitting observed in the IR spectrum close to this cluster size;[11] work is in progress along these lines.

The second, less academic, problem we address here is the characterization of a weak feature recently observed in the infra-red spectrum of carbon dioxide molecules embedded in helium droplets,[12] namely, a weak satellite band (SB) accompanying a sharp R(0) rovibrational line. The presence of such a satellite band is no surprise. The high precision afforded by RQMC in the calculation of CFs[9] allows one to clearly detect more $J = 1$ rotational states on top of the dominant free-rotor-like excitation, which originates the R(0) transition. Analysis of the $\mathscr{C}(\tau)$ CFs computed for $CO_2$ in He clusters[23] indeed shows that the second lowest excitation energy is about 20 K, with a spectral weight of a few percent, in agreement with the experiment.[12] The study of its nature, on the other hand, is intriguing. Because its energy is above the bulk He roton gap, the effective rotor is expected to couple to localized states, rather than to bulk-like excitations.[24] He-related vibrational modes in the first solvation shell are natural candidates. However, it has been suggested[12] that a key role could be played by azimuthal rotations of He atoms in the first solvation shell. In a highly simplified model[25] of two coupled planar rotors, representing the molecule and an azimuthal ring of $N$ He atoms, the Bose symmetry requires that the ring can only have rotational excitations with angular momentum $l$ in multiples of $N$. The molecular rotor then has angular momentum $j = N \pm 1$, to yield a total $J = 1$, and the second $J = 1$ excitation is symmetry-constrained to have relatively high energy. With a value of $N$ of about 6 or 7 adequate to the first solvation shell of $CO_2$, the model gives excitation energies[12] comparable to the measured SB.

We want now to get some insight by applying the SAITCF approach. The simulation details and the choice of the inter-particle potentials are the same as those in ref 23. We already mentioned that we do find a (1,0) state with an energy of ∼20 K and a spectral weight of a few percent. If the ring model were indeed relevant to the SB, we would expect at least one state, with a value of the molecular angular momentum $j$ in the range of 5−8[12] and significant spectral weight, degenerate with the SB. Furthermore, we would not expect many such states outside of this $j$ range; this is not strictly needed (see the caption of Table 1 for the meaning of the spectral weight in the SAITCF approach), but it would be strongly suggestive. Finally, we would expect all of the above to be significantly size-dependent in the small cluster regime because there have to be enough He atoms to build the azimuthal ring. The excitation energies of $CO_2@He_N$ clusters with total angular momentum $J = 1$, extracted from $\mathscr{C}_{jl}$, are shown in Figure 1 for $N = 20$ and in
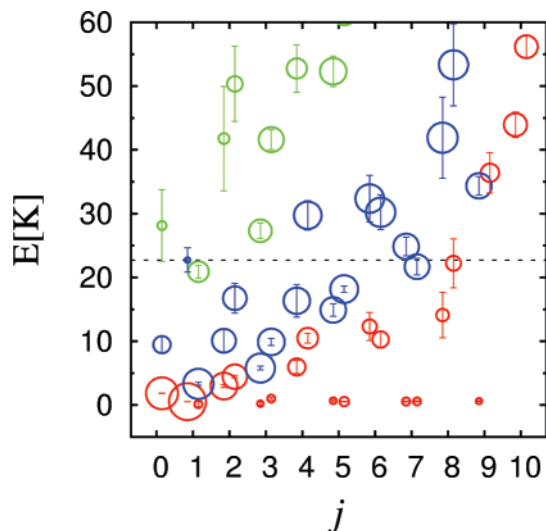
**Figure 1.** Excitation energies of a $CO_2@He_{20}$ cluster extracted from the CFs $\mathcal{G}_{jl}$ as a function of $j$. The total angular momentum is $J = 1$, and $l = j \pm 1$. For clarity, the $l = j \pm 1$ data have been slightly right/left shifted. Each energy is represented by a circle whose area is proportional to its spectral weight. For each $(j,l)$, the spectral weights of the vertically stacked energies (red, blue, and green from lowest to highest) add to one. A horizontal dashed line is drawn at the energy of the satellite band evaluated from the dipole−dipole correlation function.
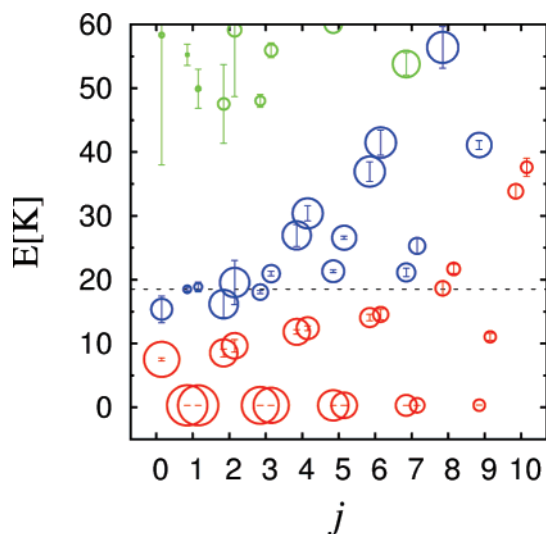


**Figure 2.** Same as that in Figure 1 but for the $CO_2@He_5$ cluster.

Figure 2 for $N = 5$. The first five He atoms form a highly localized equatorial "donut" in the minimum of the He−$CO_2$ potential, whereas $N = 20$ corresponds to one full solvation shell.[23]

We consider the $N = 20$ case first. The value ($j = 1$, $l = 0$) corresponds to the standard correlation function used in previous work[23] (the data reported here, however, all come from a new simulation, in which all of the CFs were obtained at once). The big circle (down to the $x$ axis on the scale of the figure) is the familiar free-rotor state, and the little circle at $E \approx 20$ K with a much larger error bar is the satellite band. Now, we sweep the $j$ range looking for more states at a nearby value of $E$. Generally speaking, there are vestiges of the $E \sim j^2$ behavior, which in the ring model places the right energy at the right $j$ value, that is, only few states of the type $|j = 1 \pm N, l = \mp N\rangle$ are contributing to the first excited state of this rotationally coupled system. This means that we expect really few (at most, one or two) rotational excitations in the vicinity of SB if the

ring model is relevant. Indeed, the energy of the SB calculated from the dipole−dipole CF, indicated by the dashed line, is close to two excited states with significant spectral weight at $j = 7$, as well as to a state with $j = 8$. Such high $j$ values of the states found at the energy of the SB are supportive of the ring model. There is also a contribution from (1,2), but overall, the picture is at least consistent with the fact that the satellite band may be characterized by significant contributions from high-$j$ rotational excitations.

The rest of the figure encodes a lot of interesting information. For instance, there are plenty of $J = 1$ rotational excitations, but most of them do not contribute to the experimentally observed spectrum. However, we do not delve into this analysis now and leave a more complete study of these (and possibly more) CFs for further investigation.

For $N = 5$, there is definitely no azimuthal ring around the molecule because all of the He atoms are rather tightly bound to the equatorial donut. The Bose symmetry argument at the basis of the ring model, applied to the equatorial donut, can affect a Q branch[26] but not the SB. Therefore, we simulated the $CO_2@He_5$ cluster to verify the size dependence of those aspects of the SB which are presumably related to high-$j$ states (we do expect a SB anyway since, in general, we never see a one-exponential decay in the CFs). Figure 2, indeed, shows that the $N = 5$ SB is degenerate (within the rather large statistical uncertainty) with several states with different $j$, those at $j = 2$ having a particularly strong spectral weight; as expected within the ring model, at this cluster size, there is not a dominance of high-$j$ states at the energy of the satellite band. However, the SB is surprisingly still close to 20 K. Furthermore, a SB at about 20 K, with no evidence of a strong characterization as a high-$j$ mode, is found for $N = 10$ as well. This would suggest that the value of the SB energy is not due to the $j^2$ behavior combined with restrictions from Bose symmetry, which is the cornerstone for its interpretation in terms of the ring model.

In summary, we find one result in favor of the ring model (namely, a clear high-$j$ characterization of the SB only at cluster sizes where the ring is fully established) and one result which could be seen as against the ring model (namely, the independence of the SB energy on the cluster size, across a range where the ring itself disappears). A more systematic study of the $N$-dependence of the SB and a calculation of its variation with the moment of inertia of the dopant molecule will fully clarify this issue.

For the time being, the present results indicate that SAITCFs will be instrumental to such a clarification and that they indeed hold the promise of being powerful tools in the simulation of the spectra of systems of interacting bosons and in their physical interpretation.

**References and Notes**

(1) Goyal, S.; Schutt, D. L.; Scoles, G. *Phys. Rev. Lett.* **1992**, *69*, 933.
(2) Toennies, J. P.; Vilesov, A. F. *Angew. Chem.* **2004**, *43*, 2622.
(3) Choi, M. Y.; Douberly, G. E.; Falconer, T. M.; Lewis, W. K.; Lindsay, C. M.; Merritt, J. M.; Stiles, P. L.; Miller, R. E. *Int. Rev. Phys. Chem.* **2006**, *25*, 15.
(4) Stienkemeier, F.; Lehmann, K. K. *J. Phys. B* **2006**, *39*, R127.
(5) Barranco, M.; Guardiola, R.; Hernandez, S.; Mayol, R.; Navarro, J.; Pi, M. *J. Low Temp. Phys.* **2006**, *142*, 1.
(6) Tang, J.; Xu, Y. J.; McKellar, A. R. W.; Jëger, W. *Science* **2002**, *297*, 2030.

Unraveling Excited States of Doped Helium Clusters

*J. Phys. Chem. A, Vol. 111, No. 49, 2007* **12753**

(7) Tang, J.; McKellar, A. R. W. *J. Chem. Phys.* **2004**, *121*, 181.

(8) Lehmann, K. K.; Scoles, G. *Science* **1998**, *279*, 2065.

(9) Moroni, S.; Sarsa, A.; Fantoni, S.; Schmidt, K. E.; Baroni, S. *Phys. Rev. Lett.* **2003**, *90*, 143401.

(10) Baroni, S.; Moroni, S. *Phys. Rev. Lett.* **1999**, *82*, 4745.

(11) Tang, J.; McKellar, A. R. W. *J. Chem. Phys.* **2003**, *119*, 754.

(12) Hoshina, H.; Lucrezi, J.; Slipchenko, M. N.; Kuyanov, K. E.; Vilesov, A. F. *Phys. Rev. Lett.* **2005**, *94*, 195301.

(13) Blume, D.; Mladenović, M.; Lewerentz, M.; Whaley, K. B. *J. Chem. Phys.* **1999**, *110*, 5789.

(14) Gubernatis, J. E.; Jarrell, M. *Phys. Rep.* **1996**, *269*, 135.

(15) Cazzato, P.; Paolini, S.; Moroni, S.; Baroni, S. *J. Chem. Phys.* **2004**, *120*, 9071.

(16) Chuaqui, C. E.; Le Roy, R. J.; McKellar, A. R. W. *J. Chem. Phys.* **1994**, *101*, 39.

(17) Chan, M.-C.; McKellar, A. R. W. *J. Chem. Phys.* **1996**, *105*, 7910.

(18) Zillich, R. E.; Paesani, F.; Kwon, Y.; Whaley, K. B. *J. Chem. Phys.* **2005**, *123*, 114301.

(19) Mikosz, A. A.; Ramilowski, J. A.; Farrelly, D. *J. Chem. Phys.* **2006**, *125*, 014312.

(20) Moszynski, R.; Korona, T.; Wormer, P. E. S.; van der Avoird, A. *J. Chem. Phys.* **1995**, *103*, 321.

(21) Heijmen, T. G. A.; Moszynski, R.; Wormer, P. E. S.; van der Avoird, A. *J. Chem. Phys.* **1997**, *107*, 9921.

(22) Škrbić, T.; Moroni, S.; Baroni, S. *J. Phys. Chem. A* **2007**, *111*, 7640.

(23) Tang, J.; McKellar, A. R. W.; Mezzacapo, F.; Moroni, S. *Phys. Rev. Lett.* **2004**, *92*, 145503.

(24) Zillich, R. E.; Kwon, Y.; Whaley, K. B. *Phys. Rev. Lett.* **2004**, *93*, 250401.

(25) Lehmann, K. K. *J. Chem. Phys.* **2001**, *114*, 4643.

(26) Draeger, E. W.; Ceperley, D. M. *Phys. Rev. Lett.* **2003**, *90*, 065301.